

# Inhibition of the Formation of the Spf1p Phosphoenzyme by $\text{Ca}^{2+}$ \*

Received for publication, September 29, 2015, and in revised form, January 27, 2016. Published, JBC Papers in Press, February 8, 2016, DOI 10.1074/jbc.M115.695122

Gerardo R. Corradi<sup>1</sup>, Nicolas A. Czysezon<sup>1</sup>, Luciana R. Mazzitelli, Nicolas Sarbia, and Hugo P. Adamo<sup>2</sup>

From the Instituto de Química y Físicoquímica Biológicas, Facultad de Farmacia y Bioquímica, Universidad de Buenos Aires, 1113 Ciudad Autónoma de Buenos Aires, Argentina

P5-ATPases are important for processes associated with the endosomal-lysosomal system of eukaryotic cells. In humans, the loss of function of P5-ATPases causes neurodegeneration. In the yeast *Saccharomyces cerevisiae*, deletion of P5-ATPase Spf1p gives rise to endoplasmic reticulum stress. The reaction cycle of P5-ATPases is poorly characterized. Here, we showed that the formation of the Spf1p catalytic phosphoenzyme was fast in a reaction medium containing ATP,  $\text{Mg}^{2+}$ , and EGTA. Low concentrations of  $\text{Ca}^{2+}$  in the phosphorylation medium decreased the rate of phosphorylation and the maximal level of phosphoenzyme. Neither  $\text{Mn}^{2+}$  nor  $\text{Mg}^{2+}$  had an inhibitory effect on the formation of the phosphoenzyme similar to that of  $\text{Ca}^{2+}$ . The  $K_m$  for ATP in the phosphorylation reaction was  $\sim 1 \mu\text{M}$  and did not significantly change in the presence of  $\text{Ca}^{2+}$ . Half-maximal phosphorylation was attained at  $8 \mu\text{M}$   $\text{Mg}^{2+}$ , but higher concentrations partially protected from  $\text{Ca}^{2+}$  inhibition. In conditions similar to those used for phosphorylation,  $\text{Ca}^{2+}$  had a small effect accelerating dephosphorylation and minimally affected ATPase activity, suggesting that the formation of the phosphoenzyme was not the limiting step of the ATP hydrolytic cycle.

P5-ATPases comprise a group of proteins that are classified as P-ATPases based on the presence of the characteristic P-ATPase motifs in their primary sequence (1, 2). P5-ATPases have been found only in eukaryotes and have been recently proposed to play an essential role in the endosomal-lysosomal system (3, 4). The yeast *Saccharomyces cerevisiae* contains two genes coding for P5-ATPases: YEL031W, coding for Spf1p (also called Cod1p), and YOR291W, coding for Ypk9. Spf1p (sensitivity to *Pichia farinosa* killer toxin) was initially isolated from a mutation protecting *Saccharomyces* from the effect of a *Pichia* toxin (5). The protein was also independently identified as required for the controlled degradation of 3-hydroxy-3-methylglutaryl coenzyme A reductase in the endoplasmic reticulum (ER)<sup>3</sup> (6). These and later

studies have shown that Spf1p is located in the yeast ER and that deletion of Spf1p leads to phenotypes related to ER stress (7–9). In humans, five genes (ATP13A1–A5) code for P5-ATPases (10). Mutations in ATP13A2 have been linked to an early onset autosomal recessive form of Parkinson disease (Kufor-Rakeb syndrome) and neuronal ceroid lipofuscinosis, whereas mutations in ATP13A4 have been associated with autism spectrum disorder (11–13).

P-ATPases are a large group of enzymes that couple the hydrolysis of ATP with the active transport of ions (14, 15). During the transport cycle, they transiently form a phosphoenzyme (EP) that plays a key role in the active transport mechanism. P-ATPases comprise a membrane domain (M) and a soluble portion with nucleotide binding (N), phosphorylation (P), and actuator (A) domains. These domains are involved in a kinase-phosphatase reaction cycle through two major conformations,  $E_1$ - $E_2$ , and the transient formation of a catalytic EP. The binding of the transported ion to the  $E_1$  form prompts the assembly of the phosphorylation site between the ATP-bound N domain and the P domain, whereas the A domain directs the occlusion of the bound ion. When the phosphorylation reaction occurs, it initially generates the high energy  $E_1$ -P intermediate and releases ADP.  $E_1$ -P then changes to  $E_2$ -P, and the A domain associates with the N-P complex and dephosphorylates the P domain. The binding of a counter transported ion is associated with the dephosphorylation of  $E_2$ -P. Finally, the cycle recommences with the transition of  $E_2$  back to  $E_1$ .

At present, the biochemical characterization of P5-ATPases is limited, and the putative transported ion has not yet been identified (16). The best characterized P5-ATPase is Spf1p. Spf1p is capable of hydrolyzing ATP and forming the catalytic EP in a relatively simple reaction medium containing no added metal ions except  $\text{Mg}^{2+}$ , a cofactor of all P-ATPases (7, 17, 18). This result suggests either that the Spf1p transported ion is already present in the reaction medium, for example  $\text{H}^+$  ions, or that Spf1p is unique in that it can spontaneously adopt an  $E_1$  conformation ready for phosphorylation by ATP. Furthermore, a substantial amount of the EP formed by Spf1p is of the  $E_1$ -P type, as indicated by its fast decomposition in the presence of ADP (17, 18).

Earlier studies based on the phenotypes generated by Spf1p deletion led to the suggestion that Spf1p may be a  $\text{Ca}^{2+}$  transporter (7, 19, 20). However, direct biochemical measurements to confirm this assumption are still lacking (21). It has been recently reported that  $\text{Ca}^{2+}$  ions stimulate the decay of the EP of HvP5A1, a homolog of Spf1p from barley (17). The aim of the present study was to examine in more detail the kinetics of the

\* This work was supported by Grant PICT 1240 from Agencia Nacional de Promoción Científica y Tecnológica, by Grant PIP 1042 from Consejo Nacional de Investigaciones Científicas y Tecnológicas, and by a research grant from Universidad de Buenos Aires. The authors declare that they have no conflicts of interest with the contents of this article.

<sup>1</sup> These authors contributed equally to this work.

<sup>2</sup> To whom correspondence should be addressed: IQUIFIB-Facultad de Farmacia y Bioquímica, Junín 956, 1113 Ciudad Autónoma de Buenos Aires, Argentina. Tel: 541-49648289, Ext. 127; Fax: 541-49625457; E-mail: hpadamo@qb.ffyb.uba.ar.

<sup>3</sup> The abbreviations used are: ER, endoplasmic reticulum; Spf1, sensitivity to *P. farinosa* killer toxin;  $\text{C}_{12}\text{E}_{10}$ , polyoxyethylene 10-lauryl ether; EP, phosphorylated enzyme.

## The Effect of $\text{Ca}^{2+}$ on the Spf1p Phosphoenzyme

formation and decomposition of the Spf1p EP and the influence of  $\text{Ca}^{2+}$ .

### Experimental Procedures

**Chemicals**—Polyoxyethylene-10-laurylether ( $\text{C}_{12}\text{E}_{10}$ ), L- $\alpha$ -phosphatidylcholine type XVI-E Sigma from fresh egg yolk, ATP (disodium salt, vanadium-free), SDS, yeast synthetic dropout medium supplement without leucine, yeast nitrogen base without amino acids, dextrose, enzymes and cofactors were obtained from Sigma. Tryptone and yeast extract were from Difco. PerkinElmer Life Sciences provided the [ $\gamma$ - $^{32}\text{P}$ ]ATP. Salts and reagents were of analytical reagent grade.

**Yeast Strain and Growth Media**—*S. cerevisiae* strain DBY 2062 (*MAT $\alpha$  his4-619 leu2-3,112*) (18) was used for expression. Yeast cells were transformed with the pMP625 vector containing a  $\text{Leu}^+$  marker and the PMAI promoter and the cDNA coding for either Spf1p or the fusion protein GFP-Spf1p. The experiments reported here were done using GFP-Spf1p, which has the same ATPase activity and maximal phosphorylation level as Spf1p (18) and allows an easy quantitation of its expression by fluorescence microscopy. The growing medium contained 6.7% yeast-nitrogen base without amino acids, 0.67% complete supplemented medium minus Leu and 2.2% dextrose.

**Purification of Spf1p**—Purified preparations of recombinant Spf1p were obtained by a procedure essentially similar to that described previously (18). Briefly, total membranes from 4 liters of yeasts expressing the GFP-Spf1p or Spf1p were isolated, and the microsomal membranes were suspended in a purification buffer containing 20 mM MOPS-K (pH 7.4 at 4 °C), 20% glycerol, 130 mM KCl, 1 mM  $\text{MgCl}_2$ , 2 mM dithiothreitol, 1 mM phenylmethylsulfonyl fluoride, homogenized in a glass homogenizer, and solubilized at 4 °C for 15 min by adding 2 g of  $\text{C}_{12}\text{E}_{10}$ /g of total membrane protein. 10 mM imidazole was added to the supernatant, and then it was loaded onto a 2-ml nickel-nitrilotriacetic acid-agarose column (Qiagen) and washed with 30 column volumes of purification buffer containing 0.05%  $\text{C}_{12}\text{E}_{10}$  and 50 mM imidazole. Finally, the protein was eluted in purification buffer containing 0.005%  $\text{C}_{12}\text{E}_{10}$  and 150 mM imidazole. The eluate fractions of higher protein content were pooled, aliquoted, and kept in liquid  $\text{N}_2$ .

**Protein Assay**—During the purification procedure, the protein concentration was estimated by the method of Bradford (22), and finally it was corrected according to the intensity of the bands after SDS-PAGE on an 8% acrylamide gel according to Laemmli (23) using bovine serum albumin as a standard and staining with Coomassie Blue.

**Phosphorylation**—The phosphorylation reaction was performed with 1.5  $\mu\text{g}$  of purified GFP-Spf1, which was phosphorylated at 4 °C in 0.25 ml of reaction buffer containing 50 mM Tris-HCl (pH 7.2), 0.5 mM EGTA,  $\text{MgCl}_2$  to give a concentration of 2 mM  $\text{Mg}^{2+}$  and the concentrations of ATP and  $\text{Ca}^{2+}$  (as  $\text{CaCl}_2$ ) indicated in each experiment. GFP-Spf1p was supplemented with 0.85  $\mu\text{g}$  of  $\text{C}_{12}\text{E}_{10}$  and 4.3  $\mu\text{g}$  of phosphatidylcholine. This suspension was mixed and preincubated for at least 5 min on ice before it was added to the reaction medium. The phosphorylation reaction started with the addition of [ $\gamma$ - $^{32}\text{P}$ ]ATP, and it was stopped after the time indicated in each experiment with 15% ice-cold trichloroacetic acid. The dena-

tured proteins were collected by centrifugation at  $20,000 \times g$  for 10 min, washed once with 5% trichloroacetic acid and 150 mM  $\text{NaH}_2\text{PO}_4$ , and washed once more with distilled water. The precipitated protein was suspended in sample buffer and separated by acidic SDS-PAGE. Slices of the gel containing the Spf1p phosphoenzyme were cut, and the radioactivity was measured in a scintillation counter. For measuring the EP decay, GFP-Spf1p was phosphorylated for 60 s at 4 °C, and then the radioactive label was diluted by adding 500  $\mu\text{M}$  of cold ATP.

**ATPase Activity**—The ATPase activity was estimated at 28 °C from the release of [ $^{32}\text{P}$ ] from [ $\gamma$ - $^{32}\text{P}$ ]ATP (24) in a final volume of 0.25 ml of "ATPase medium" containing, 50 mM Tris-HCl (pH 7.2), 0.5 mM EGTA, 5 mM  $\text{N}_3\text{Na}$ , 2 mM  $\text{MgCl}_2$ , 30  $\mu\text{M}$  ATP, and 1  $\mu\text{g}$  of GFP-Spf1 in 50  $\mu\text{l}$  of elution buffer. The GFP-Spf1 protein was supplemented with 0.85  $\mu\text{g}$  of  $\text{C}_{12}\text{E}_{10}$  and 4.3  $\mu\text{g}$  of phosphatidylcholine, the suspension was mixed and preincubated for at least 5 min on ice before being added to the reaction medium. The reaction was initiated by the addition of ATP and terminated by acid denaturation.

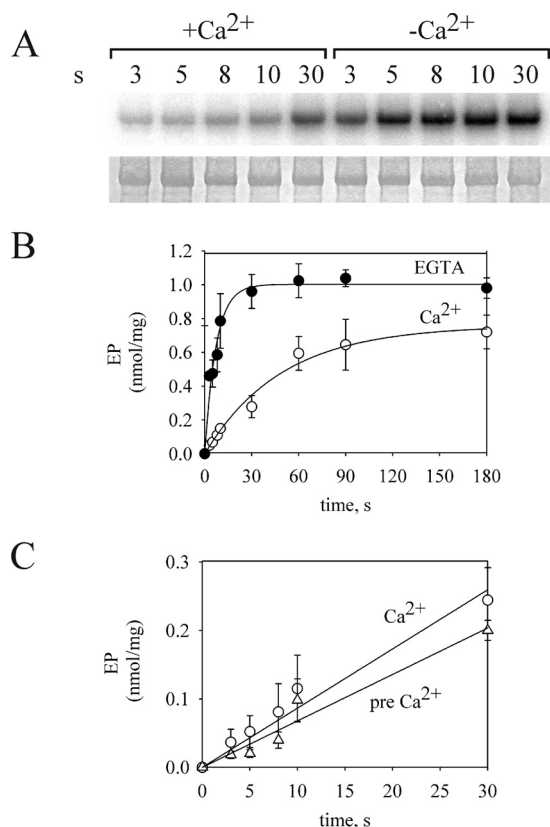
**Data Analysis**—Except where indicated, the data points represent the average values of two or three independent determinations performed with different purified protein preparations. Best fitting values of the parameters and their S.E. were obtained by fitting the equations indicated in the legends of the figures to the experimental data using the SigmaPlot 10 scientific data analysis and graphing software (Systat Software Inc., CA) for Windows.

### Results

**Phosphorylation of Spf1p by ATP**—Purified Spf1p was preincubated in a medium containing 0.5 mM EGTA and 2 mM  $\text{Mg}^{2+}$  and phosphorylated by the addition of 0.5  $\mu\text{M}$  [ $\gamma$ - $^{32}\text{P}$ ]ATP at 4 °C. The results in Fig. 1 show that, in this condition, the reaction was fast and reached a maximal amount of EP of  $\sim 1$  nmol/mg of protein at  $\sim 30$  s. The value of the apparent phosphorylation rate constant ( $k_p$ ), obtained by fitting a monoexponential rise to maximum function, was  $0.14 \text{ s}^{-1}$ . When the phosphorylation was initiated by adding ATP and  $\text{CaCl}_2$  to give 100  $\mu\text{M}$   $\text{Ca}^{2+}$  in the phosphorylation medium, the levels of EP were significantly lower and increased slowly with time ( $k_p = 0.02 \text{ s}^{-1}$ ) up to a maximal level of 0.75 nmol/mg of protein. At short times of phosphorylation the level of EP was  $\sim 8$  times higher in the absence than in the presence of  $\text{Ca}^{2+}$ . The initial rate of phosphorylation ( $v_0$ ) is a function of the amount of  $\text{E}_1$  and the apparent constant of the reaction ( $k_p$ ).

$$v_0 = k_p[E_1] \quad (\text{Eq. 1})$$

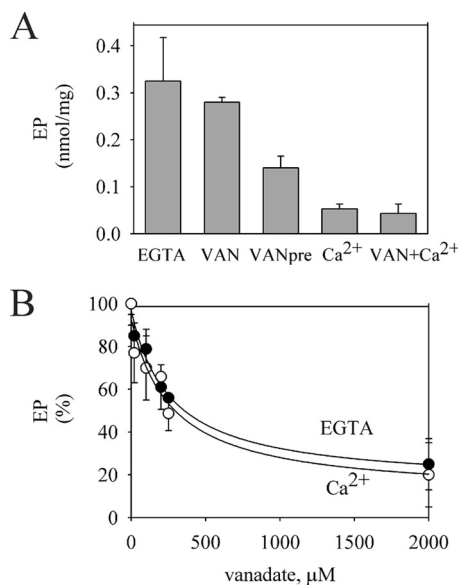
The effect of  $\text{Ca}^{2+}$  decreasing the level of EP was readily observed when  $\text{Ca}^{2+}$  was added together with ATP, suggesting that it did not involve a change in the amount of  $\text{E}_1$ . As shown in Fig. 1C, preincubation of the enzyme with  $\text{Ca}^{2+}$  before the beginning of phosphorylation resulted in a minimal decrease of the phosphorylation rate compared with that attained when  $\text{Ca}^{2+}$  was only present during phosphorylation. These results suggest that  $\text{Ca}^{2+}$  directly decreased the apparent rate constant of phosphorylation, as indicated in Equation 1.



**FIGURE 1. Time course of EP formation.** *A*, acidic gel electrophoresis of phosphorylated GFP-Spf1p showing the radioactivity (*top panel*) or the Coomassie Blue staining (*bottom panel*). 1.5  $\mu\text{g}$  of GFP-Spf1p was suspended at 4 °C in a medium containing 2 mM  $\text{Mg}^{2+}$  and 0.5 mM EGTA. The reaction was started by adding 0.5  $\mu\text{M}$  ATP plus 0.5 mM EGTA or 0.5  $\mu\text{M}$  ATP plus enough  $\text{CaCl}_2$  to give a final concentration of 100  $\mu\text{M}$   $\text{Ca}^{2+}$ . *B*, EP levels quantified as described under "Experimental Procedures." The data points are the averages from three experiments. *Error bars* show the standard deviation. ●, 0.5 mM EGTA; ○, 100  $\mu\text{M}$   $\text{Ca}^{2+}$ . The data were fitted by an exponential equation with the following parameters, in the absence of  $\text{Ca}^{2+}$   $EP_{\text{max}} = 1.00 \pm 0.03$  nmol/mg, and  $k_p = 0.14 \pm 0.01$  s $^{-1}$ , and in the presence of  $\text{Ca}^{2+}$ ,  $EP_{\text{max}} = 0.75 \pm 0.04$  nmol/mg, and  $k_p = 0.020 \pm 0.002$  s $^{-1}$ . *C*, the phosphorylation was done in conditions similar to *B* except that either the enzyme was suspended in a reaction medium with 0.5 mM EGTA, and  $\text{Ca}^{2+}$  was added together with ATP (*circles*), or the enzyme was preincubated in a reaction medium with  $\text{Ca}^{2+}$  for 5 min at 4 °C before starting the phosphorylation (*triangles*). The data points are the averages from two experiments. *Error bars* show the standard deviation.

Further information on the effect of  $\text{Ca}^{2+}$  was obtained by comparing its effects with those of vanadate (Fig. 2). Vanadate, a well known inhibitor of P-ATPases, binds to the nonphosphorylatable  $E_2$  conformation, displacing the equilibrium between  $E_2$  and  $E_1$  toward the former. In contrast with the effect of  $\text{Ca}^{2+}$ , the formation of EP was significantly inhibited only when vanadate was in contact with the enzyme before phosphorylation. Moreover, when the enzyme was preincubated with vanadate, its apparent affinity as an inhibitor of phosphorylation was similar in the absence and in the presence of  $\text{Ca}^{2+}$ . These results indicate that  $\text{Ca}^{2+}$  did not affect the  $E_2$ - $E_1$  equilibrium.

**Dependence of the Rate of Phosphorylation on the Concentration of  $\text{Ca}^{2+}$** —The level of EP at 5 s of phosphorylation was determined in medium containing increasing concentrations of  $\text{Ca}^{2+}$ . As shown in Fig. 3A, the yield of EP decreased rapidly with a  $K_i$  of  $\sim 0.2$   $\mu\text{M}$   $\text{Ca}^{2+}$  and then seemed to remain constant at concentrations higher than 100  $\mu\text{M}$   $\text{Ca}^{2+}$ .



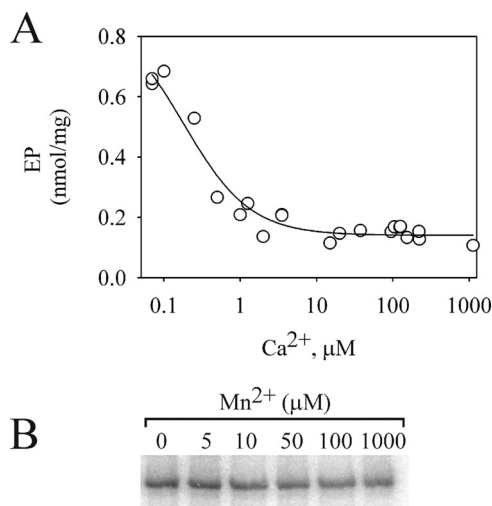
**FIGURE 2. Comparison of the effects of  $\text{Ca}^{2+}$  and vanadate on the EP formation.** *A*, 1.5  $\mu\text{g}$  of GFP-Spf1p was suspended at 4 °C in a medium containing 2 mM  $\text{Mg}^{2+}$  and 0.5 mM EGTA, and the phosphorylation was started by adding 0.5  $\mu\text{M}$  ATP (EGTA); 0.5  $\mu\text{M}$  ATP plus 200  $\mu\text{M}$  vanadate (VAN); 0.5  $\mu\text{M}$  ATP plus 100  $\mu\text{M}$   $\text{Ca}^{2+}$  ( $\text{Ca}^{2+}$ ); or 0.5  $\mu\text{M}$  ATP, 200  $\mu\text{M}$  vanadate, and 100  $\mu\text{M}$   $\text{Ca}^{2+}$  (VAN+ $\text{Ca}^{2+}$ ). The bar (VANpre) shows the level of EP formed in conditions similar to (VAN) except that the enzyme was preincubated for 5 min at 4 °C with 200  $\mu\text{M}$  vanadate before starting the phosphorylation. The reaction time was 5 s. The values are the average from two experiments. *Error bars* show the standard deviation. *B*, GFP-Spf1p was suspended at 4 °C in a medium containing 2 mM  $\text{Mg}^{2+}$  and 0.5 mM EGTA and the indicated concentration of vanadate. The phosphorylation was started by adding 0.5  $\mu\text{M}$  ATP (*filled circles*) or 0.5  $\mu\text{M}$  ATP plus 100  $\mu\text{M}$   $\text{Ca}^{2+}$  (*empty circles*). The value of EP in each condition in the absence of vanadate was taken as 100%. The data points are the averages from three experiments, and the *error bars* show the standard deviation. The *lines* represents the best fit to the data given by the hyperbolic equation  $EP = EP_0 + EP_m[\text{vanadate}]/(K_i + [\text{vanadate}])$ , with the following parameters, in the absence of  $\text{Ca}^{2+}$ ,  $EP_0 = 15 \pm 7\%$ ,  $K_i = 267 \pm 75$   $\mu\text{M}$  and  $EP_m = 81 \pm 7\%$  and in 100  $\mu\text{M}$   $\text{Ca}^{2+}$ ,  $EP_0 = 10 \pm 13\%$ ,  $K_i = 274 \pm 144$   $\mu\text{M}$ , and  $EP_m = 82 \pm 14\%$ .

Fig. 3B shows the effect of increasing concentrations of  $\text{Mn}^{2+}$  on the level of EP. Somewhat lower levels of EP were observed as  $\text{Mn}^{2+}$  concentration increased from 0 to 1 mM. However, the effect of  $\text{Mn}^{2+}$  on EP was weaker than that of  $\text{Ca}^{2+}$ .

**Apparent Affinity for ATP**—One possible explanation of the inhibitory effect of  $\text{Ca}^{2+}$  on the rate constant of phosphorylation could be a decrease in the affinity for ATP. To test this hypothesis, the level of EP was measured at increasing concentrations of ATP (Fig. 4). In the presence of 0.5 mM EGTA and 2 mM  $\text{Mg}^{2+}$ , the level of EP at 5 s of phosphorylation increased rapidly with the concentration of ATP in the range of 0–30  $\mu\text{M}$ , following a hyperbolic curve with  $K_m = 1$   $\mu\text{M}$ . The addition of ATP plus  $\text{CaCl}_2$  to give a final  $\text{Ca}^{2+}$  concentration of 100  $\mu\text{M}$  lowered the levels of EP obtained at all the concentrations of ATP tested. The estimated  $K_m$  for ATP in the presence of  $\text{Ca}^{2+}$  was 0.9  $\mu\text{M}$ . Thus,  $\text{Ca}^{2+}$  did not significantly change the apparent affinity for ATP at the high affinity site.

**Apparent Affinity for  $\text{Mg}^{2+}$** — $\text{Mg}^{2+}$  is a common cofactor of all P-ATPases. To test the effect of  $\text{Mg}^{2+}$  on the phosphorylation of Spf1p, we measured the level of EP at increasing concentrations of  $\text{Mg}^{2+}$ . In the presence of 0.5 mM EGTA, the EP at 5 s of phosphorylation increased with the concentration of  $\text{Mg}^{2+}$ , reaching a maximal level at  $\sim 100$   $\mu\text{M}$  (Fig. 5). When  $\text{Ca}^{2+}$  was

## The Effect of $\text{Ca}^{2+}$ on the Spf1p Phosphoenzyme



**FIGURE 3. Dependence of the EP formation with the concentration of  $\text{Ca}^{2+}$  and  $\text{Mn}^{2+}$ .** A, 1.5  $\mu\text{g}$  of GFP-Spf1p was suspended at 4 °C in a medium containing 2 mM  $\text{Mg}^{2+}$ , 0.5 mM EGTA and increasing concentrations of  $\text{CaCl}_2$  to give the indicated concentrations of  $\text{Ca}^{2+}$  in the final reaction medium. The reaction was started by adding 30  $\mu\text{M}$  ATP and terminated after 5 s. The data points shown are measurements from three independent experiments. The line represents the best fit to the data given by the hyperbolic equation  $EP = EP_0 + EP_{Ca} [\text{Ca}]/(K_i + [\text{Ca}])$ , with the following parameters  $EP_0 = 0.14 \pm 0.01$  nmol/mg,  $K_i = 0.18 \pm 0.04$   $\mu\text{M}$ , and  $EP_{Ca} = 0.74 \pm 0.06$  nmol/mg. B, GFP-Spf1p was suspended at 4 °C in a medium containing 2 mM  $\text{Mg}^{2+}$  and the indicated concentrations of  $\text{Mn}^{2+}$  and phosphorylated by the addition of 30  $\mu\text{M}$  ATP.

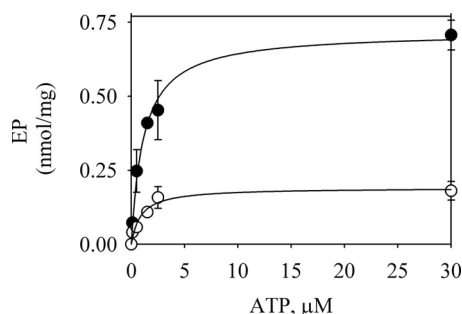


**FIGURE 4. ATP dependence of EP formation.** 1.5  $\mu\text{g}$  of GFP-Spf1p was suspended at 4 °C in a medium containing 2 mM  $\text{Mg}^{2+}$ , 0.5 mM EGTA, and the phosphorylation was started by adding ATP (filled circles) or ATP plus  $\text{CaCl}_2$  to give 100  $\mu\text{M}$   $\text{Ca}^{2+}$  (empty circles). The reaction time was 5 s. The concentrations of ATP indicated correspond to the final concentration in the reaction medium. The data points are the averages from two experiments, and the error bars show the standard deviation. The lines represent the best fit to the data given by a hyperbolic equation with  $EP = EP_{\text{max5}} [\text{ATP}]/(K_m + [\text{Ca}^{2+}])$  with the following parameters: without  $\text{Ca}^{2+}$ ,  $EP_{\text{max5}} = 0.72 \pm 0.03$  nmol/mg,  $K_m = 1.1 \pm 0.1$   $\mu\text{M}$ , with  $\text{Ca}^{2+}$ ,  $EP_{\text{max5}} = 0.19 \pm 0.01$  nmol/mg, and  $K_m = 0.9 \pm 0.3$   $\mu\text{M}$ .

added to the phosphorylation medium, the EP levels were lower, increased with mM concentrations of  $\text{Mg}^{2+}$ , and reached lower maximal levels than that obtained in the absence of  $\text{Ca}^{2+}$ . The estimated  $\text{Mg}^{2+}$  concentration for half-maximal activation of the phosphorylation reaction was  $\sim 0.28$  mM at 0.2  $\mu\text{M}$   $\text{Ca}^{2+}$  and 1.25 mM at 100  $\mu\text{M}$   $\text{Ca}^{2+}$ .

**Effects of  $\text{Ca}^{2+}$  on Dephosphorylation**— $\text{Ca}^{2+}$  has been shown to promote the dephosphorylation of Hvp5A1, a barley homolog of Spf1p (17). Here, we examined the effects of  $\text{Ca}^{2+}$  on the decay of EP in conditions similar to those used for the phosphorylation reaction. To this end, Spf1p was phosphorylated in medium with EGTA and no added  $\text{CaCl}_2$ , and the decay of EP was followed both in the absence of  $\text{Ca}^{2+}$  and after the addition

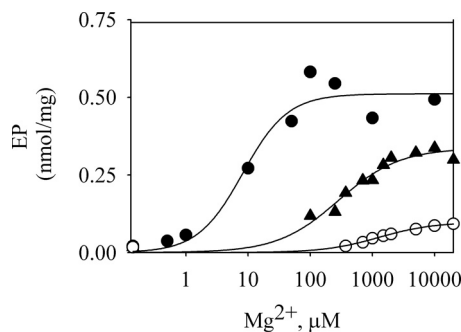


**FIGURE 5.  $\text{Mg}^{2+}$  dependence of EP formation.** 1.5  $\mu\text{g}$  of GFP-Spf1p was suspended at 4 °C in a medium containing 0.5 mM EGTA and enough  $\text{MgCl}_2$  to give the indicated final  $\text{Mg}^{2+}$  concentrations in the phosphorylation medium. The phosphorylation was started by adding 30  $\mu\text{M}$  ATP (filled circles), 30  $\mu\text{M}$  ATP plus 0.2  $\mu\text{M}$   $\text{Ca}^{2+}$  (filled triangles), or 30  $\mu\text{M}$  ATP plus 100  $\mu\text{M}$   $\text{Ca}^{2+}$  (empty circles). The reaction time was 5 s. The data points shown are measurements from five independent experiments. The lines represent the best fit to the data given by the Hill equation. The estimated values of  $K_{Mg}$  were 8, 280, and 1250  $\mu\text{M}$  for no  $\text{Ca}^{2+}$ , 0.2  $\mu\text{M}$   $\text{Ca}^{2+}$ , and 100  $\mu\text{M}$   $\text{Ca}^{2+}$ , respectively.

of  $\text{CaCl}_2$  to give 100  $\mu\text{M}$   $\text{Ca}^{2+}$ . The time courses of dephosphorylation were biphasic (Fig. 6). The addition of  $\text{Ca}^{2+}$  at the start of dephosphorylation increased  $\sim 2$ -fold the rate of the rapid component, whereas the slow component was minimally affected.

**ATPase Activity**—In previous studies, we did not detect a significant effect of  $\text{Ca}^{2+}$  on the ATPase activity of Spf1p (18). However, because here we found that  $\text{Ca}^{2+}$  changed the level and kinetics of EP, we reexamined its effects on ATPase by using a low concentration of ATP (30  $\mu\text{M}$ ) and short reaction times similar to those of the phosphorylation experiments. In these conditions, ATPase activity in the presence of 0.5 mM EGTA was slightly higher than that in the presence of 100  $\mu\text{M}$   $\text{Ca}^{2+}$  (Fig. 7).

## Discussion

Here, we investigated the formation and decay of the catalytic phosphorylated intermediate of Spf1p in the presence and in the absence of  $\text{Ca}^{2+}$ . In agreement with previous studies (7, 17, 18), we found that Spf1p readily accepted the  $\gamma$ -P from ATP, provided  $\text{Mg}^{2+}$  was present in the medium. The phosphorylation reaction attained maximal rate and maximal levels of EP in medium containing enough EGTA to reduce the concentration of  $\text{Ca}^{2+}$  to less than 0.1  $\mu\text{M}$ . The estimated values of the rate constants for phosphorylation for Spf1p are in the range of those reported for other P-ATPases (25, 26). On the other hand, the maximal level of EP measured in different preparations of the purified protein allows estimating a stoichiometry of near 0.1 mol EP/mol of protein. Although this value is far from the theoretical stoichiometry of 1:1, it is close to the values reported for other P-ATPases like those of the P4 type (27). In addition, the amount of EP detected may be underestimated because of the inactivation of the protein during the purification process, the presence of a small amount of contaminant proteins in the purified preparation, and the decomposition of EP during the acidic gel electrophoresis. In any case, our results indicate that the absence of  $\text{Ca}^{2+}$  stabilizes Spf1p in its phosphorylated form.

**Effects of  $\text{Ca}^{2+}$  on Phosphorylation**—When the phosphorylation reaction took place in the presence of  $\text{Ca}^{2+}$ , the apparent rate of phosphorylation and the maximum level of EP

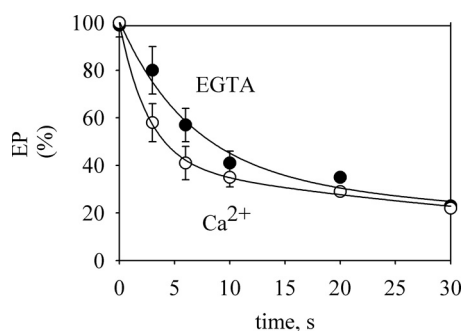


FIGURE 6. **Time course of EP decay.** GFP-Spf1p was phosphorylated for 60 s at 4 °C in a medium containing 2 mM  $\text{Mg}^{2+}$ , 0.5 mM EGTA, and 0.5  $\mu\text{M}$  ATP, and the dephosphorylation was measured after diluting the radioactive label with 500  $\mu\text{M}$  of cold ATP or 500  $\mu\text{M}$  of cold ATP plus enough  $\text{CaCl}_2$  to give 100  $\mu\text{M}$   $\text{Ca}^{2+}$ . The lines represent the best fit to the data given by an equation of double exponential decay. The data points are the averages from two experiments. Error bars show the standard deviation.

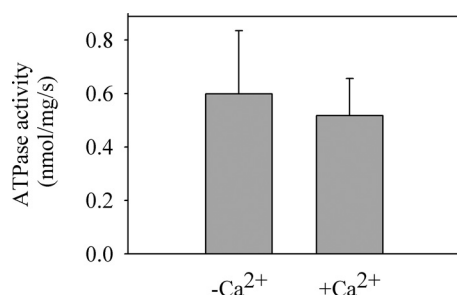


FIGURE 7. **Effect of  $\text{Ca}^{2+}$  on the ATPase activity.** The ATPase activity of GFP-Spf1p was measured as described under "Experimental Procedures" at 28 °C for 20 s in a reaction medium containing 30  $\mu\text{M}$  ATP, 2 mM  $\text{Mg}^{2+}$ , 0.5 mM EGTA with (+Ca), or without (-Ca)  $\text{CaCl}_2$  to give 100  $\mu\text{M}$   $\text{Ca}^{2+}$ . The data points are the averages from three experiments. Error bars show the standard deviation.

decreased. The effect of  $\text{Ca}^{2+}$  was fast and readily observed when  $\text{Ca}^{2+}$  was added together with ATP, suggesting that  $\text{Ca}^{2+}$  directly inhibited the phosphorylation reaction. Moreover,  $\text{Ca}^{2+}$  did not affect the  $\text{E}_2\text{-E}_1$  equilibrium, as indicated by (i) the lack of effect of the preincubation of the enzyme with  $\text{Ca}^{2+}$  before starting phosphorylation and (ii) the lack of effect of  $\text{Ca}^{2+}$  on the apparent affinity for the  $\text{E}_2$  ligand vanadate. In contrast, the experiments with vanadate suggest that the enzyme can be forced to adopt the  $\text{E}_2$  conformation by preincubation with vanadate, as indicated by the lower yield of EP observed in this condition.

Half-maximal inhibition of phosphorylation by  $\text{Ca}^{2+}$  occurred at a physiological concentration range. Additionally, the observed inhibition seemed to be a specific effect of  $\text{Ca}^{2+}$  because other divalent metals such as  $\text{Mg}^{2+}$  did not inhibit the phosphorylation reaction at any of the concentrations tested. The levels of EP were slightly decreased by  $\text{Mn}^{2+}$ , suggesting that  $\text{Mn}^{2+}$  may substitute  $\text{Ca}^{2+}$  with lower efficiency. However, we have previously found that  $\text{Mn}^{2+}$  decreases Spf1p ATPase activity (18), a result that does not support the proposed role of Spf1p as a  $\text{Mn}^{2+}$  transporter (28).

The ATP dependence of the phosphorylation reaction indicates that Spf1p reacts with ATP with high affinity, as expected for the catalytic ATP site of a P-ATPase, and that it was not significantly changed by  $\text{Ca}^{2+}$ . As reported for other P-ATPases, we found that the rate of phosphorylation of Spf1p depends on the concentration of  $\text{Mg}^{2+}$  (26, 29). In the absence

of  $\text{Ca}^{2+}$ , the phosphorylation rate increased with the concentrations of  $\text{Mg}^{2+}$  in the micromolar range. Interestingly, the amount of  $\text{Mg}^{2+}$  needed to activate phosphorylation increased in the presence of  $\text{Ca}^{2+}$ , and high  $\text{Mg}^{2+}$  partially protected from  $\text{Ca}^{2+}$  inhibition.

For the mechanism of  $\text{Ca}^{2+}$  inhibition of EP formation, at least two possibilities could be considered. First,  $\text{Ca}^{2+}$  may compete with  $\text{Mg}^{2+}$  at the catalytic site of Spf1p, replacing the activating effect of  $\text{Mg}^{2+}$  with less efficiency. Such a competition occurs in other P-ATPases, with varying degree of catalytic efficiency (30, 31). Furthermore, if the inhibitory species were  $\text{Ca}^{2+}$  in complex with ATP, the affinity of Spf1p for  $\text{Ca}^{2+}$ -ATP should be extremely high, because it can be estimated that, in the conditions used for the phosphorylation reaction, more than 85% of ATP was bound to  $\text{Mg}^{2+}$ . Alternatively, the inhibition of Spf1p phosphorylation by  $\text{Ca}^{2+}$  may involve a separate  $\text{Ca}^{2+}$  site on the protein. Modulatory  $\text{Ca}^{2+}$  sites have been identified in the nucleotide domain of other P-ATPases (32). Actually, the nucleotide domain of P5-ATPases exhibits some unique amino acid motifs that may be relevant for the formation and stability of the Spf1p EP (17, 33).

**Effects of  $\text{Ca}^{2+}$  on Dephosphorylation**—Dephosphorylation involved both a fast and a slow component. We found that  $\text{Ca}^{2+}$  had a small effect accelerating the fast phase of dephosphorylation by  $\sim 2$ -fold. This type of biphasic dephosphorylation kinetics has already been described in other P-ATPases (34, 35) and may represent the fast decomposition of the preexistent  $\text{E}_2\text{P}$  followed by a slower decomposition of the  $\text{E}_2\text{P}$  formed from  $\text{E}_1\text{P}$ . If this were the case, our results would indicate that  $\text{Ca}^{2+}$  accelerates  $\text{E}_2\text{P}$  decay. On the other hand, because a substantial amount of the phosphorylated Spf1p is  $\text{E}_1\text{P}$ , the possibility that  $\text{Ca}^{2+}$  promotes the reaction of  $\text{E}_1\text{P}$  with the ADP produced cannot be discarded. Further studies are needed to discriminate between these possibilities. Moreover, by using yeast membrane preparations, Sørensen *et al.* (17) showed that  $\text{Ca}^{2+}$  induces a spontaneous decay of the recombinant plant P5A-ATPase HvP5A1 EP. These authors showed that  $\text{Ca}^{2+}$  exerted this effect with relatively low affinity ( $K_i = \sim 250 \mu\text{M}$ ) but was very effective in reducing EP, a fact that might have been helped by the ADP-producing hexokinase-glucose system used to deplete ATP and thus stop phosphorylation. In contrast, our present results showed that the most prominent effect of  $\text{Ca}^{2+}$  was directly inhibiting EP formation and that the effect of  $\text{Ca}^{2+}$  accelerating dephosphorylation was smaller. This is consistent with the lower level of EP detected at steady state in the presence of  $\text{Ca}^{2+}$ . An interesting hypothesis that may explain the differences between our results and those reported previously is the modulation of the effect of  $\text{Ca}^{2+}$  by detergents and lipids. Indeed, the signaling lipids phosphatidic acid and phosphatidylinositol 3,5-bisphosphate have been recently shown to increase the phosphorylation of the closely related P5B-ATPase ATP13A2 (36).

**Effects of  $\text{Ca}^{2+}$  on the ATPase Activity of Spf1p**—Spf1p ATPase activity, measured in conditions similar to those used for phosphorylation, was less affected by  $\text{Ca}^{2+}$  than expected on the basis on its effect on the formation of EP. This result suggests that the phosphorylation reaction is not limiting ATPase activity. This is in agreement with the fact that a sub-

## The Effect of Ca<sup>2+</sup> on the Spf1p Phosphoenzyme

stantial fraction of the Spf1p EP is E<sub>1</sub>P and does not transit to E<sub>2</sub>P (17, 18). In our hands, the slow phase of dephosphorylation did not seem to change with Ca<sup>2+</sup>, which might be related to the lack of stimulation of ATPase activity. We believe that the effect of Ca<sup>2+</sup> on Spf1p may depend on the temperature of the assay, the presence of other modulators, different lipid environments, and potential interacting partners that are unknown at present. This requires further investigation.

**Significance of the Effects of Ca<sup>2+</sup> on the Function of Spf1p**—Because earlier studies indicated a connection between Spf1p and Ca<sup>2+</sup> homeostasis (6, 7), it is tempting to speculate on the potential relevance of a Ca<sup>2+</sup> modulation of the Spf1p function. Moreover, Ca<sup>2+</sup> plays an important role in membrane trafficking, a process also affected by the function of P5-ATPases (3). We have considered the possibility that the observed effects of Ca<sup>2+</sup> are the consequence of its action as a transported counterion in the catalytic cycle of Spf1p. However, based on the results presented here and the comparison with the behavior of other P-ATPases, we believe that this option is unlikely. Because Ca<sup>2+</sup> directly inhibited the ATP phosphorylation of Spf1p, it presumably acted from the cytosol. In contrast, a counterion is expected to act from the luminal side of the membrane. In addition, if Ca<sup>2+</sup> increased the turnover of EP by acting as a counterion, it should be pumped out from the lumen of the ER. Although functional reconstitution of Spf1p into liposomes has not yet been reported, it should be soon available for a direct testing of Spf1p transporting activity. Nevertheless, Ca<sup>2+</sup> may modulate the functions of Spf1p even if it is not transported. Indeed, the catalytic subunit of P4-ATPase Drs2p interacts with its Cdc50p subunit preferentially when it is phosphorylated (27). Our results indicate that at the low concentrations of Ca<sup>2+</sup> present in the cytosol at resting conditions, Spf1p would be stabilized in the phosphorylated form, and this might influence its interaction with other protein partners. In this line, the effects of Ca<sup>2+</sup> on the formation of the catalytic EP of Spf1p may be part of a signaling pathway from the cytosol to the ER.

**Author Contributions**—G. R. C. and N. A. C. designed, performed, and analyzed the experiments. L. R. M. and N. S. performed the experiments and contributed to the preparation of the figures. H. P. A. designed the study, analyzed the experiments, and wrote the paper. All authors analyzed the results and approved the final version of the manuscript.

**Acknowledgment**—We thank R. Y. Hampton for the generous gift of the cDNA sequence coding for the Spf1 protein.

### References

1. Palmgren, M. G., Axelsen, K. B. (1998) Evolution of P-type ATPases. *Biochim. Biophys. Acta* **1365**, 37–45
2. Sørensen, D. M., Buch-Pedersen, M. J., and Palmgren, M. G. (2010) Structural divergence between the two subgroups of P5 ATPases. *Biochim. Biophys. Acta* **1797**, 846–855
3. van Veen, S., Sørensen, D. M., Hølemans, T., Hølen, H. W., Palmgren, M. G., and Vangheluwe, P. (2014) Cellular function and pathological role of ATP13A2 and related P-type transport ATPases in Parkinson's disease and other neurological disorders. *Front. Mol. Neurosci.* **7**, 48
4. Perrett, R. M., Alexopoulou, Z., and Tofaris, G. K. (2015) The endosomal pathway in Parkinson's disease. *Mol. Cell Neurosci.* **66**, 21–28

5. Suzuki, C., and Shimma, Y. I. (1999) P-type ATPase Spf1 mutants show a novel resistance mechanism for the killer toxin SMKT. *Mol. Microbiol.* **32**, 813–823
6. Cronin, S. R., Khoury, A., Ferry, D. K., and Hampton, R. Y. (2000) Regulation of HMG-CoA reductase degradation requires the P-type ATPase Cod1p/Spf1p. *J. Cell Biol.* **148**, 915–924
7. Cronin, S. R., Rao, R., and Hampton, R. Y. (2002) Cod1p/Spf1p is a P-type ATPase involved in ER function and Ca<sup>2+</sup> homeostasis. *J. Cell Biol.* **157**, 1017–1028
8. Tipper, D. J., and Harley, C. A. (2002) Yeast genes controlling responses to topogenic signals in a model transmembrane protein. *Mol. Biol. Cell* **13**, 1158–1174
9. Vashist, S., Frank, C. G., Jakob, C. A., and Ng, D. T. (2002) Two distinctly localized P-type ATPases collaborate to maintain organelle homeostasis required for glycoprotein processing and quality control. *Mol. Biol. Cell* **13**, 3955–3966
10. Schultheis, P. J., Hagen, T. T., O'Toole, K. K., Tachibana, A., Burke, C. R., McGill, D. L., Okunade, G. W., and Shull, G. E. (2004) Characterization of the P5 subfamily of P-type transport ATPases in mice. *Biochem. Biophys. Res. Commun.* **323**, 731–738
11. Ramirez, A., Heimbach, A., Gründemann, J., Stiller, B., Hampshire, D., Cid, L. P., Goebel, I., Mubaidin, A. F., Wriekat, A. L., Roeper, J., Al-Din, A., Hillmer, A. M., Karsak, M., Liss, B., Woods, C. G., Behrens, M. I., and Kubisch, C. (2006) Hereditary parkinsonism with dementia is caused by mutations in ATP13A2, encoding a lysosomal type 5 P-type ATPase. *Nat. Genet.* **38**, 1184–1191
12. Kwasnicka-Crawford, D. A., Carson, A. R., Roberts, W., Summers, A. M., Rehnström, K., Järvelä, I., and Scherer, S. W. (2005) Characterization of a novel cation transporter ATPase gene (ATP13A4) interrupted by 3q25-q29 inversion in an individual with language delay. *Genomics* **86**, 182–194
13. Bras, J., Verloes, A., Schneider, S. A., Mole, S. E., and Guerreiro, R. J. (2012) Mutation of the parkinsonism gene ATP13A2 causes neuronal ceroid-lipofuscinosis. *Hum. Mol. Genet.* **21**, 2646–26650
14. Toyoshima, C., and Inesi, G. (2004) Structural basis of ion pumping by Ca<sup>2+</sup>-ATPase of the sarcoplasmic reticulum. *Annu. Rev. Biochem.* **73**, 269–292
15. Palmgren, M. G., and Nissen, P. (2011) P-ATPases. *Annu. Rev. Biophys.* **40**, 243–266
16. Sørensen, D. M., Hølen, H. W., Hølemans, T., Vangheluwe, P., and Palmgren, M. G. (2015) Towards defining the substrate of orphan P5A-ATPases *Biochim. Biophys. Acta* **1850**, 524–535
17. Sørensen, D. M., Møller, A. B., Jakobsen, M. K., Jensen, M. K., Vangheluwe, P., Buch-Pedersen, M. J., and Palmgren, M. G. (2012) Ca<sup>2+</sup> induces spontaneous dephosphorylation of a novel P5A-type ATPase. *J. Biol. Chem.* **287**, 28336–28348
18. Corradi, G. R., de Tezanos Pinto, F., Mazzitelli, L. R., and Adamo, H. P. (2012) Shadows of an absent partner: ATP hydrolysis and phosphoenzyme turnover of the Spf1 (sensitivity to *Pichia farinosa* killer toxin) P5-ATPase. *J. Biol. Chem.* **287**, 30477–30484
19. Vallipuram, J., Grenville, J., and Crawford, D. A. (2010) The E646D-ATP13A4 mutation associated with autism reveals a defect in calcium regulation. *Cell. Mol. Neurobiol.* **30**, 233–246
20. Lustoza, A. C., Palma, L. M., Façanha, A. R., Okorokov, L. A., and Okorokova-Façanha A. L. (2011) P5A-type ATPase Cta4p is essential for Ca<sup>2+</sup> transport in the endoplasmic reticulum of *Schizosaccharomyces pombe*. *PLoS One* **6**, e27843
21. de Tezanos Pinto, F., Corradi, G. R., and Adamo, H. P. (2011) The human P<sub>5B</sub>-ATPase ATP13A2 is not a Ca<sup>2+</sup> transporting pump. *J. Life Sci.* **5**, 1–6
22. Bradford, M. M. (1976) A rapid and sensitive method for the quantitation of microgram quantities of protein utilizing the principle of protein-dye binding. *Anal. Biochem.* **72**, 248–254
23. Laemmli, U. K. (1970) Cleavage of structural proteins during the assembly of the head of bacteriophage T4. *Nature* **227**, 680–685
24. Richards, D. E., Rega, A. F., and Garrahan, P. J. (1978) Two classes of site for ATP in the Ca<sup>2+</sup>-ATPase from human red cell membranes. *Biochim. Biophys. Acta* **511**, 194–201
25. Vestergaard, A. L., Coleman, J. A., Lemmin, T., Mikkelsen, S. A., Molday, L. L., Vilsen, B., Molday, R. S., Dal Peraro, M., and Andersen, J. P. (2014)

- Critical roles of isoleucine-364 and adjacent residues in a hydrophobic gate control of phospholipid transport by the mammalian P4-ATPase ATP8A2. *Proc. Natl. Acad. Sci. U.S.A.* **111**, E1334–E1343
26. Garrahan, P. J., and Rega, A. F. (1978) Activation of partial reactions of the  $\text{Ca}^{2+}$  ATPase from human red cells by  $\text{Mg}^{2+}$  and ATP. *Biochim. Biophys. Acta* **513**, 59–65
  27. Lenoir, G., Williamson, P., Puts, C. F., and Holthuis, J. C. (2009) Cdc50p plays a vital role in the ATPase reaction cycle of the putative aminophospholipid transporter Drs2p. *J. Biol. Chem.* **284**, 17956–17967
  28. Cohen, Y., Megyeri, M., Chen, O. C., Condomitti, G., Riezman, I., Loizides-Mangold, U., Abdul-Sada, A., Rimon, N., Riezman, H., Platt, F. M., Futerman, A. H., and Schuldiner, M. (2013) The yeast P5 type ATPase, Spf1, regulates manganese transport into the endoplasmic reticulum. *PLoS One* **8**, e85519
  29. Adamo, H. P., Rega, A. F., and Garrahan, P. J. (1988) Pre-steady-state phosphorylation of the human red cell  $\text{Ca}^{2+}$ -ATPase. *J. Biol. Chem.* **263**, 17548–17554
  30. Caride, A. J., Rega, A. F., and Garrahan (1986) The reaction of  $\text{Mg}^{2+}$  with the  $\text{Ca}^{2+}$ -ATPase from human red cell membranes and its modification by  $\text{Ca}^{2+}$ . *Biochim. Biophys. Acta* **863**, 165–177
  31. Mendlein, J., and Sachs, G. (1989) The substitution of calcium for magnesium in  $\text{H}^+, \text{K}^+$ -ATPase catalytic cycle: evidence for two actions of divalent cations. *J. Biol. Chem.* **264**, 18512–18519
  32. Ekberg, K., Pedersen, B. P., Sørensen, D. M., Nielsen, A. K., Veierskov, B., Nissen, P., Palmgren, M. G., and Buch-Pedersen, M. J. (2010) Structural identification of cation binding pockets in the plasma membrane proton pump. *Proc. Natl. Acad. Sci. U.S.A.* **107**, 21400–21405
  33. Møller, A. B., Asp, T., Holm, P. B., and Palmgren, M. G. (2008) Phylogenetic analysis of P5 P-type ATPases, a eukaryotic lineage of secretory pathway pumps. *Mol. Phylogenet. Evol.* **46**, 619–634
  34. Hobbs, A. S., Albers, R. W., Froehlich, J. P., and Heller, P. F. (1985) ADP stimulates hydrolysis of the ADP-insensitive phosphoenzyme in  $\text{Na}^+ \cdot \text{K}^+$ -ATPase and  $\text{Ca}^{2+}$ -ATPase. *J. Biol. Chem.* **260**, 2035–2037
  35. Nakamura, Y., Kurzmack, M., and Inesi, G. (1986) Kinetic effects of calcium and ADP on the phosphorylated intermediate of sarcoplasmic reticulum ATPase. *J. Biol. Chem.* **261**, 3090–3097
  36. Holemans, T., Sørensen, D. M., van Veen, S., Martin, S., Hermans, D., Kemmer, G. C., Van den Haute, C., Baekelandt, V., Günther Pomorski, T., Agostinis, P., Wuytack, F., Palmgren, M., Eggermont, J., and Vangheluwe, P. (2015) A lipid switch unlocks Parkinson's disease-associated ATP13A2. *Proc. Natl. Acad. Sci. U.S.A.* **112**, 9040–9045